PAPER

Finite-thickness effect of the fluids on bubbles and spikes in Richtmyer–Meshkov instability for arbitrary Atwood numbers

To cite this article: Wanhai LIU *et al* 2019 *Plasma Sci. Technol.* **21** 025001

Plasma Sci. Technol. **21** (2019) 025001 (7pp) https://doi.org/10.1088/2058-6272/aaee0c

Finite-thickness effect of the fluids on bubbles and spikes in Richtmyer–Meshkov instability for arbitrary Atwood numbers

Wanhai LIU (刘万海)[1], **Changping YU** (于长平)[2,5], **Pei WANG** (王裴)[3], **Zheng FU** (付峥)[3], **Lili WANG** (王丽丽)[3] **and Yulian CHEN** (陈玉莲)[4]

[1] Research Center of Computational Physics, Mianyang Normal University, Mianyang 621000, People's Republic of China
[2] LHD, Institute of Mechanics, Chinese Academy of Sciences, Beijing 100190, People's Republic of China
[3] Institute of Applied Physics and Computational Mathematics, Beijing 100190, People's Republic of China
[4] Mechanical and Electrical Engineering Department, Lanzhou Resources and Environment Voc-Tech College, Lanzhou 730021, People's Republic of China

E-mail: cpyu@imech.ac.cn

Received 21 July 2018, revised 31 October 2018
Accepted for publication 2 November 2018
Published 13 December 2018

Abstract

This paper investigates the finite-thickness effect of two superimposed fluids on bubbles and spikes in Richtmyer–Meshkov instability (RMI) for arbitrary Atwood numbers by using the method of the small parameter expansion up to the second order. When the thickness of the two fluids tends to be infinity, our results can reproduce the classical results where RMI happens at the interface separating two semi-infinity-thickness fluids of different densities. It is found that the thickness has a large influence on the amplitude evolution of bubbles and spikes compared with those in classical RMI. Based on the thickness relationship of the two fluids, the thickness effect on bubbles and spikes for four cases is discussed. The thickness encourages (or reduces) the growth of bubbles or spikes, depending on not only Atwood number, but also the relationship of the thickness ratio of the heavy and light fluids, which is explicitly determined in this paper.

Keywords: Richtmyer–Meshkov instability, bubbles and spikes, finite-thickness

(Some figures may appear in colour only in the online journal)

1. Introduction

Richtmyer–Meshkov instability (RMI) usually happens at two cases. One is that when an incident shock colliding with a corrugated interface which separates two fluids of variable density, the interface is prone to RMI [1, 2], the other is that RMI is activated by the variable vorticities at the interface, either deposited at first or imposed by other sources [3, 4]. RMI is very important to the fields, such as inertial confinement fusion and astrophysical problems [5, 6]. In a wide range of engineering, geophysical, and astrophysical flows, the RMI is one of the triggering events that, in many cases, can lead to large-scale turbulent mixing, see in the recent two-part comprehensive reviews [7, 8] where the concerns over the past 140 years on Rayleigh–Taylor [9–18] and RM instabilities have been introduced in details. The Rayleigh–Taylor instability (RTI) occurs when a light fluid supports or accelerates a heavy one. The classical RTI and RMI are usually considered to happen on the interface separating two fluids with semi-infinity thickness. However, the RTI and RMI generally appear when the two fluids are with finite-thickness. In RTI, finite-thickness effect [15–18] of the fluids was widely concerned.

A large number of the studies on RMI have been performed, such as some experiments [19] and numerical simulations [20–22] on the growth rate, and other theories [23–32] using different explicit methods. Most of these express great concern over the earlier growth rate of the

[5] Author to whom any correspondence should be addressed.

interface, and with the asymptotic behavior of the RMI interface fingers: bubbles and spikes which are, respectively, formed by the light fluid entering into the heavy one, and by the heavy fluid traveling in the light fluid.

For incompressible and inviscid fluids, within the third-order framework, the weakly nonlinear solution for the interface of the initial cosine single-mode perturbation is given as $\eta(x, t) = \eta_1 \cos(kx) + \eta_2 \cos(2kx) + \eta_3 \cos(3kx)$. The amplitudes of the first three harmonics [30] are

$$\eta_1 = (tv_0 + a_0) - \frac{1}{24}[(4A^2 + 1)tv_0 + 3a_0]k^2t^2v_0^2, \quad (1a)$$

$$\eta_2 = \frac{1}{2}Akt^2v_0^2, \quad (1b)$$

$$\eta_3 = \frac{1}{8}[(4A^2 - 1)tv_0 - 3a_0]k^2t^2v_0^2, \quad (1c)$$

where $k = 2\pi/\lambda$, λ, a_0 and v_0 are, respectively, the wave number, wavelength, amplitude, and velocity of the initial perturbation at the interface, Atwood number $A = (\rho_h - \rho_l)/(\rho_h + \rho_l)$ with ρ_h (ρ_l) being the density of the heavy (light) fluid, and t is time. As for detailed discussions of the first three harmonics, see [31].

In fact, RMI happens at the interface separating two finite-thickness fluids. However, investigations on this aspect are not much. Reference [33] presented a linear analytic theory of RMI induced by a shock as an impulsive acceleration in an arbitrary number N of stratified fluids. In this paper, we predict a weakly nonlinear theory up to the second order and research the amplitude evolution of bubbles and spikes for RMI with finite-thickness fluids.

2. Theoretical framework and explicit results up to the second order

In the Cartesian coordinate system (x, y, z), the heavy fluid with finite-thickness d_2 is overlapped on the light fluid with finite-thickness d_1, and there exist three interfaces. Set the middle interface between them to be at $y = 0$ planar, and the upper interface of the heavy fluid and the lower interface of the light fluid are, respectively, located at $y = d_2$ and $y = -d_1$ planar. For some reasons, these three interfaces are not always planar, but with perturbations. To better seek the finite-thickness effect, the initial interfaces are given to be

$$y = \eta_l(x, t = 0) = -d_1 + \varepsilon_1 \cos(kx), \quad (2a)$$

$$y = \eta_u(x, t = 0) = d_2 + \varepsilon_3 \cos(kx), \quad (2b)$$

$$y = \eta_m(x, t = 0) = 0 + \varepsilon_2 \cos(kx), \quad (2c)$$

where ε_1, ε_2 and ε_3 are, respectively, perturbation amplitudes of these three interfaces. Here, the amplitudes of the perturbation are far less than their wavelength, namely max (ε_1, ε_2, ε_3) $\ll \lambda$, and the regions $y > d_2$ and $y < -d_1$ are vacuum. The initial velocity distributions of these three interfaces are

$$\frac{\partial \eta_i(x, t)}{\partial t}|_{t=0} = v_j \cos(kx), \quad (3)$$

with $i = l, m, u$ corresponding to $j = 1, 2, 3$.

Because of the perturbations of the amplitudes and velocities above, these three interfaces $\eta_l(x, t)$, $\eta_m(x, t)$ and $\eta_u(x, t)$ evolving with time should satisfy conditions of the kinematic and pressure boundary.

For the lower (upper) interface, it is a free boundary: the normal velocities of the interface and light (heavy) fluid should keep continuous, while at the middle interface, in the normal direction of this interface the velocities of the light and heavy fluids should keep continuous. Therefore, the conditions of the kinematic boundary are

$$\frac{\partial \eta_l}{\partial t} + \frac{\partial \eta_l}{\partial x}\frac{\partial \phi_l}{\partial x} - \frac{\partial \phi_l}{\partial y} = 0 \quad \text{at} \quad y = \eta_l(x, t), \quad (4a)$$

$$\frac{\partial \eta_u}{\partial t} + \frac{\partial \eta_u}{\partial x}\frac{\partial \phi_h}{\partial x} - \frac{\partial \phi_h}{\partial y} = 0 \quad \text{at} \quad y = \eta_u(x, t), \quad (4b)$$

$$\frac{\partial \eta_m}{\partial t} + \frac{\partial \eta_m}{\partial x}\frac{\partial \phi_l}{\partial x} - \frac{\partial \phi_l}{\partial y} = 0 \quad \text{at} \quad y = \eta_m(x, t), \quad (4c)$$

$$\frac{\partial \eta_m}{\partial t} + \frac{\partial \eta_m}{\partial x}\frac{\partial \phi_h}{\partial x} - \frac{\partial \phi_h}{\partial y} = 0 \quad \text{at} \quad y = \eta_m(x, t), \quad (4d)$$

where ϕ_l and ϕ_h are velocity potentials of the light fluid and heave fluid, respectively. The ϕ_l and ϕ_h should obey Laplace equation,

$$\left(\frac{\partial^2}{\partial x^2} + \frac{\partial^2}{\partial y^2}\right)\phi_i = 0 \quad \text{in two fluids } (i = l, h). \quad (5)$$

According to Bernoulli equation, the pressure of the light or heavy fluid without gravitational acceleration is

$$p_i = -\rho_i\left[\frac{\partial \phi_i}{\partial t} + \frac{1}{2}(\nabla \phi i)^2\right] + f_i(t), \quad (6)$$

where $f_i(t)$ is an arbitrary function of time. At these three interfaces, the pressure should keep continuous. Therefore, the conditions of the equilibrium pressure are written as

$$-\rho_l\left[\frac{\partial \phi_l}{\partial t} + \frac{1}{2}(\nabla \phi l)^2\right] + f_l(t) = 0 \quad \text{at} \quad y = \eta_l(x, t), \quad (7a)$$

$$-\rho_h\left[\frac{\partial \phi_h}{\partial t} + \frac{1}{2}(\nabla \phi h)^2\right] + f_u(t) = 0 \quad \text{at} \quad y = \eta_u(x, t), \quad (7b)$$

$$\rho_l\left[\frac{\partial \phi_l}{\partial t} + \frac{1}{2}(\nabla \phi l)^2\right] - \rho_h\left[\frac{\partial \phi_h}{\partial t} + \frac{1}{2}(\nabla \phi h)^2\right] + f_m(t) = 0 \quad \text{at} \quad y = \eta_m(x, t). \quad (7c)$$

Under the framework of the second-order weakly nonlinear theory, the interfaces and velocity potentials at time t normalized by wave number k can be expressed as

$$\hat{\eta}_l(x, t) = \sigma L_{1,1}(t)\cos(kx) + \sigma^2 L_{2,2}(t)\cos(2kx) - \delta_1, \quad (8a)$$

$$\hat{\eta}_u(x, t) = \sigma U_{1,1}(t)\cos(kx) + \sigma^2 U_{2,2}(t)\cos(2kx) + \delta_2, \quad (8b)$$

$$\hat{\eta}_m(x, t) = \sigma \eta_{1,1}(t)\cos(kx) + \sigma^2 \eta_{2,2}(t)\cos(2kx), \quad (8c)$$

$$\phi_l(x, t) = \sigma \cos(kx)[a_{1,1}(t)e^{ky} + c_{1,1}(t)e^{-ky}] + \sigma^2 \cos(2kx)[a_{2,2}(t)e^{2ky} + c_{2,2}(t)e^{-2ky}], \quad (8d)$$

$$\phi_h(x, t) = \sigma \cos(kx)[b_{1,1}(t)e^{ky} + d_{1,1}(t)e^{-ky}] + \sigma^2 \cos(2kx)[b_{2,2}(t)e^{2ky} + d_{2,2}(t)e^{-2ky}], \quad (8e)$$

where the normalized parameter $\sigma = \min(k\varepsilon_1, k\varepsilon_2, k\varepsilon_3) \ll 1$, and normalized finite thicknesses of the two fluids $\delta_j = kd_j$ $(j = 1, 2)$. It should be noted that the velocity potentials ϕ_l and ϕ_h have satisfied Laplace equation (5), and the functions of the interfaces have the relations $\hat{\eta}_i(x, t) = k\eta_i(x, t)$ $(i = l, u, m)$.

Substitute equations (8*a*)–(8*e*) into equations (4*a*)–(4*d*) and (7*a*)–(7*c*), and replace y in the equations with corresponding interface η_i $(i = l, u, \text{or } m)$ expressed above. The final equations containing x and σ are obtained.

To further obtain the mth-order $(m > 0)$ equations just including the terms of σ^m, we need to expand the left hand sides of these seven final equations in Maclaurin series of σ. Here, the zeroth order equations, considering the effect of arbitrary function $f(t)$, can be satisfied automatically. Therefore the first-, and second-order equations together with the initial conditions (2*a*)–(2*c*) and (3) can be solved successively. For simplicity, at the special case where $\varepsilon_1 = \varepsilon_3 = 0$ (there are no perturbations at the free boundaries $y = \eta_l$ and $y = \eta_u$) and $v_1 = v_2 = v_3 = v_0$, we give the results

$$\eta_{1,1}(t) = \frac{1}{\sigma}(tv_0 + \varepsilon_2), \tag{9a}$$

$$\eta_{2,2}(t) = \frac{B_2}{2B_1\sigma^2}kt^2v_0^2, \tag{9b}$$

where the coupling factors B_1 and B_2 are

$$B_1 = A(-\mathrm{e}^{4\delta_1}) + \mathrm{e}^{4\delta_2}(A + \mathrm{e}^{4\delta_1}) - 1, \tag{10a}$$

$$\begin{aligned} B_2 = {} & \mathrm{e}^{2(\delta_1+\delta_2)}(A - 1)[4\cosh(\delta_1) - 3]\cosh(2\delta_2) \\ & + \mathrm{e}^{2(\delta_1+\delta_2)}[(A + 1)(4\cosh(\delta_2) - 3) \\ & - 2A\cosh(2\delta_2)]\cosh(2\delta_1), \end{aligned} \tag{10b}$$

just related to δ_1, δ_2 and A. It is found that the effect of the finite-thickness fluids has not an influence on the linear amplitude $\sigma\eta_{1,1}(t)$ of the fundamental mode, but on the second harmonic $\sigma^2\eta_{2,2}(t)$. As a result, one can obtain the middle interface as

$$\eta_m(x, t) = \eta_1\cos(kx) + \eta_2\cos(2kx). \tag{11}$$

It should be noted that when the thickness $\delta_1 \to \infty$ and $\delta_2 \to \infty$, the ratio of the B_2/B_1 will tend to be $-A$, and the middle interface will reproduce the classical evolutional interface (up to the second order) separating two semi-infinite-thickness fluids.

3. The finite-thickness effect on bubbles and spikes

For the sake of better investigation on the finite-thickness influence, one needs to normalize the expression of the middle interface by using the parameters k, ε_2 and v_0. Letting the both sides of the expression (11) multiplied by k, and denoting $X = kx$, $T = ktv_0$, $\hat{\varepsilon} = k\varepsilon_2$, and $\hat{\eta} = k\eta$, one can obtain the normalized expression of the middle interface

$$\hat{\eta}_{\mathrm{m}}(X, T) = \hat{\eta}_1(T)\cos X + \hat{\eta}_2(T)\cos 2X, \tag{12}$$

where the amplitudes of the first two harmonics are

$$\hat{\eta}_1(T) = T + \hat{\varepsilon}, \tag{13a}$$

$$\hat{\eta}_2(T) = \frac{1}{2}\frac{B_2}{B_1}T^2. \tag{13b}$$

One can find that the evolutional interface are influenced by the factors of not only Atwood number A, the initial amplitude of the interface perturbations $\hat{\varepsilon}$, but also the finite-thickness δ_1 and δ_2. Of course, theses factors can also influence the amplitude evolution of the bubbles and spikes. The normalized amplitudes of the bubbles and spikes A_{b} and A_{s} can be expressed as

$$A_b = \hat{\eta}_m(0, T), \tag{14a}$$

$$A_s = \hat{\eta}_m(\pi, T). \tag{14b}$$

In the following discussion, the normalized initial amplitude of the interface perturbation is fixed as $\hat{\varepsilon} = 1/1000$, and the cases of Atwood numbers $A = 0.2$, $A = 0.8$ and $A = 0.95$ are selected in this paper. The finite-thickness effect is in our consideration for the cases: (1) when $\delta_2 \to \infty$, the finite-thickness δ_1 varies; (2) when $\delta_1 \to \infty$, the finite-thickness δ_2 varies; (3) $\delta_1 = \delta_2$ varies; (4) the variable ratios of the δ_2/δ_1 with $\delta_1 = 1$, which are, respectively, shown in figures 1–4.

Figure 1 does not consider the finite-thickness effect of the heavy fluid (i.e. $\delta_2 \to \infty$), but the light one. It is found that the finite-thickness δ_1 has a larger influence on spikes and bubbles for smaller Atwood number than larger one. The finite-thickness δ_1 reduces the growth of the bubbles and accelerates that of the spikes for $A = 0.2$, $A = 0.8$ and $A = 0.95$. The influence of the finite-thickness δ_1 is more obvious with the larger time in the weakly nonlinear stage. Also, the smaller the δ_1 is, the stronger the influence on fingers (bubbles and spikes) is. However, for the fixed time, the amplitude of the spike is always larger than that of the bubble.

Figure 2 shows the influence of the finite-thickness δ_2 on the bubble and the spike. It is found that the finite-thickness δ_2 has a larger influence on bubbles and spikes for $A = 0.2$, $A = 0.8$ and $A = 0.95$. Whatever A is small or large, different δ_2 always strengthens the growth of the bubble and constrains that of the spike. This role of the thickness makes the spikes does not always go faster than the bubble, especially for smaller Atwood number. For the case $A = 0.2$ and $\delta_2 = 0.5$, the amplitude of the bubble is larger than that of the spike with time.

Figure 3 gives the case of the two fluids with the same finite-thickness $\delta_1 = \delta_2$. It is found that the finite-thickness plays a role of helping growth of the bubble and reducing that of the spike for different A, resulting in the almost same growth of the bubble and the spike for smaller A. This can be seen from the lines for $\delta_1 = \delta_2 = 0.1$: the amplitude of the bubble is nearly the same as that of the spike for $A = 0.2$, $A = 0.8$ or $A = 0.95$.

The influence of the finite-thickness ratio of δ_2/δ_1 on amplitudes of the bubble and the spike is shown in figure 4. For $A = 0.2$, $A = 0.8$ and $A = 0.95$, one can find that the effects of the finite-thickness ratio are nearly the same. When the ratio is larger than 1, the growth of the bubble is restrained, while the spike is encouraged; when the ratio is less than 1, the growth of the bubble is accelerated, while the

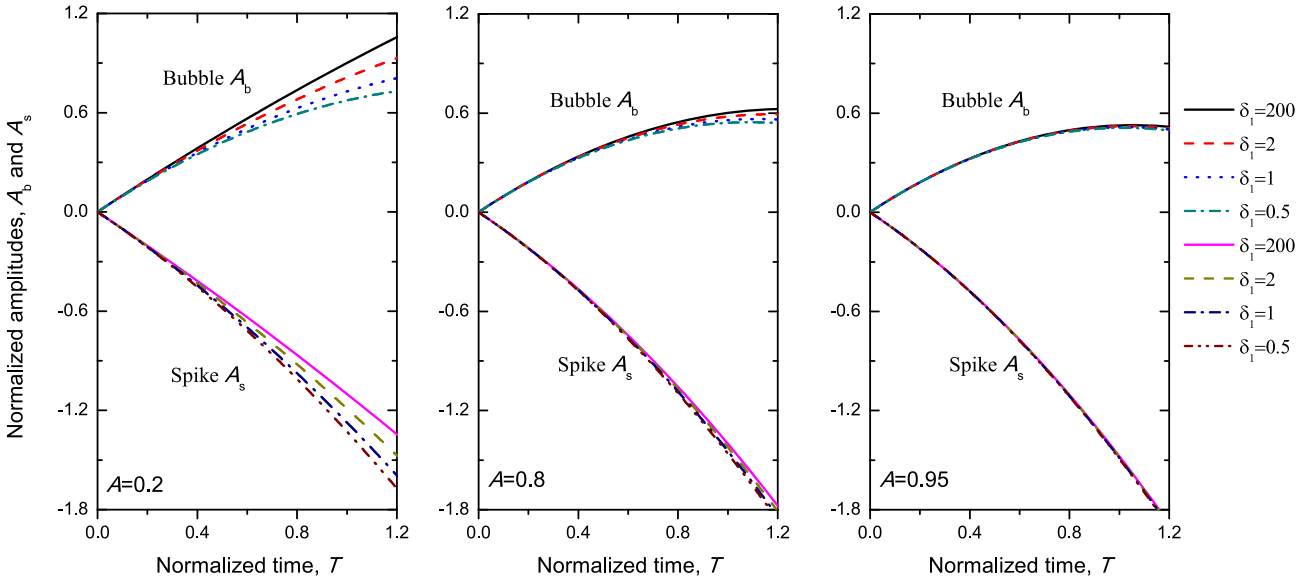

Figure 1. Normalized amplitudes of bubbles and spikes of the middle interface versus normalized time $T = kv_0t$ for different finite-thickness δ_1 of the light fluid and Atwood numbers $A = 0.2$ (left), $A = 0.8$ (middle) and $A = 0.95$ (right). The initial amplitude of the perturbation is $\hat{\varepsilon} = 1/1000$, and the finite-thickness $\delta_2 \to \infty$.

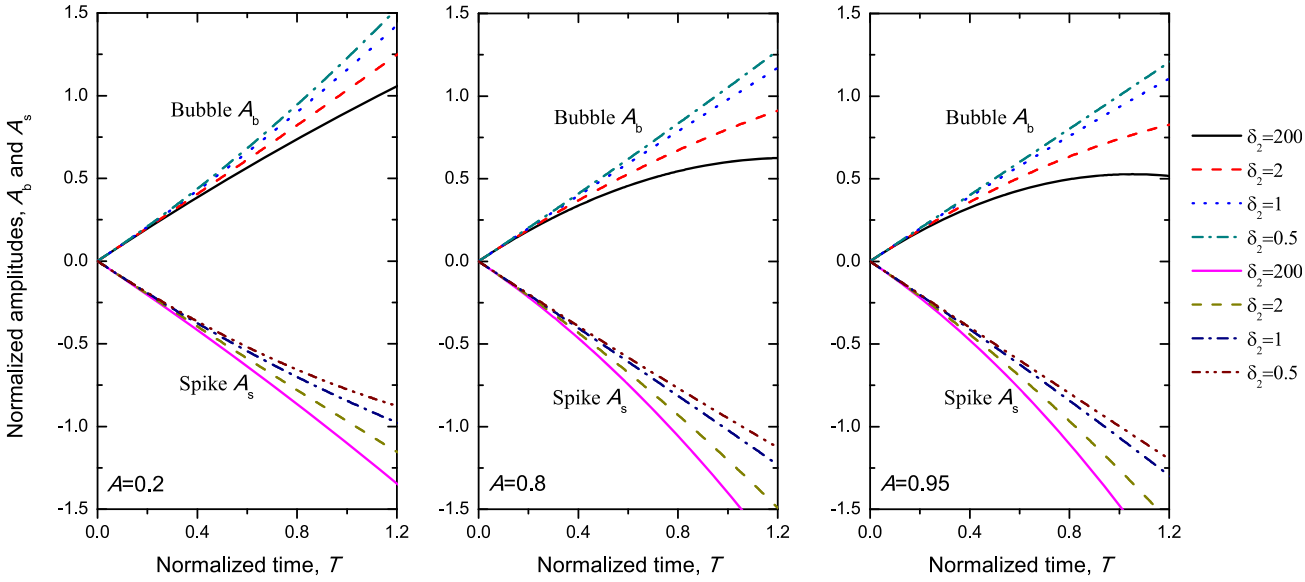

Figure 2. Normalized amplitudes of bubbles and spikes of the middle interface versus normalized time $T = kv_0t$ for different finite-thickness δ_2 of the heavy fluid and Atwood numbers $A = 0.2$ (left), $A = 0.8$ (middle) and $A = 0.95$ (right). The initial amplitude of the perturbation is $\hat{\varepsilon} = 1/1000$, and the finite-thickness $\delta_1 \to \infty$.

spike is reduced. That is, when the finite-thickness of the heavy fluid is larger than that of the light fluid, the growth of the bubble is constrained, but the spike is accelerated; when the finite-thickness of the light fluid is larger than that of the heavy fluid, the growth of the bubble is accelerated, but the spike is reduced.

From the discussion above, it is found that the finite-thickness of either the light fluid or the heavy fluid plays an important role to the growth of the bubble and the spike. The finite-thickness is less, the amplitude of the bubble and the spike grows faster or slower, depending on Atwood number. The effect of the finite-thickness of the fluids on the bubble and the spike can be concluded in the following table.

In table 1, the symbol 'bubble ↑' denotes the bubble moving to the heavy fluid, and 'spikes ↓' denotes the spike moving to the light fluid; the '↓' denotes the finite-thickness δ_1 or δ_2 decreasing; and the ⇑ (⇓) shows the strengthening (constraining) effect of the finite-thickness fluids on bubbles or spikes. This table shows that in these five cases, just two cases (1 and 4a) are in accordance with the classical, while the other three cases (2, 3 and 4b) may be not.

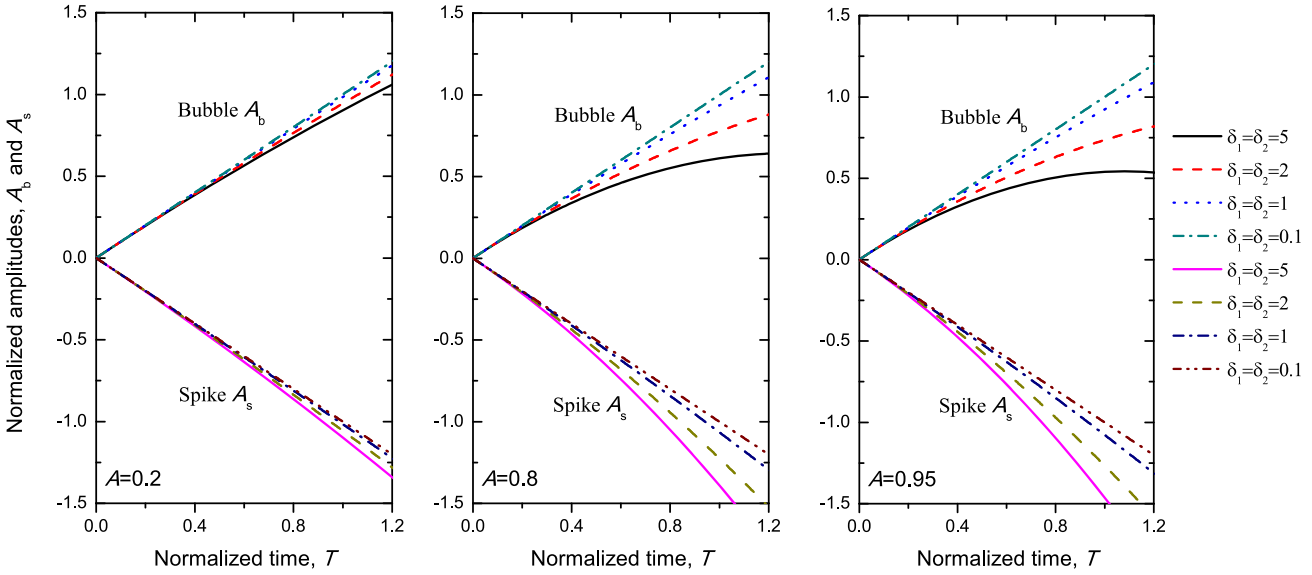

Figure 3. Normalized amplitudes of bubbles and spikes of the middle interface versus normalized time $T = kv_0t$ for different finite-thickness $\delta_1 = \delta_2 = 5$, 2, 1, 0.1 and Atwood numbers $A = 0.2$ (left), $A = 0.8$ (middle) and $A = 0.95$ (right). The initial amplitude of the perturbation is $\hat{\varepsilon} = 1/1000$.

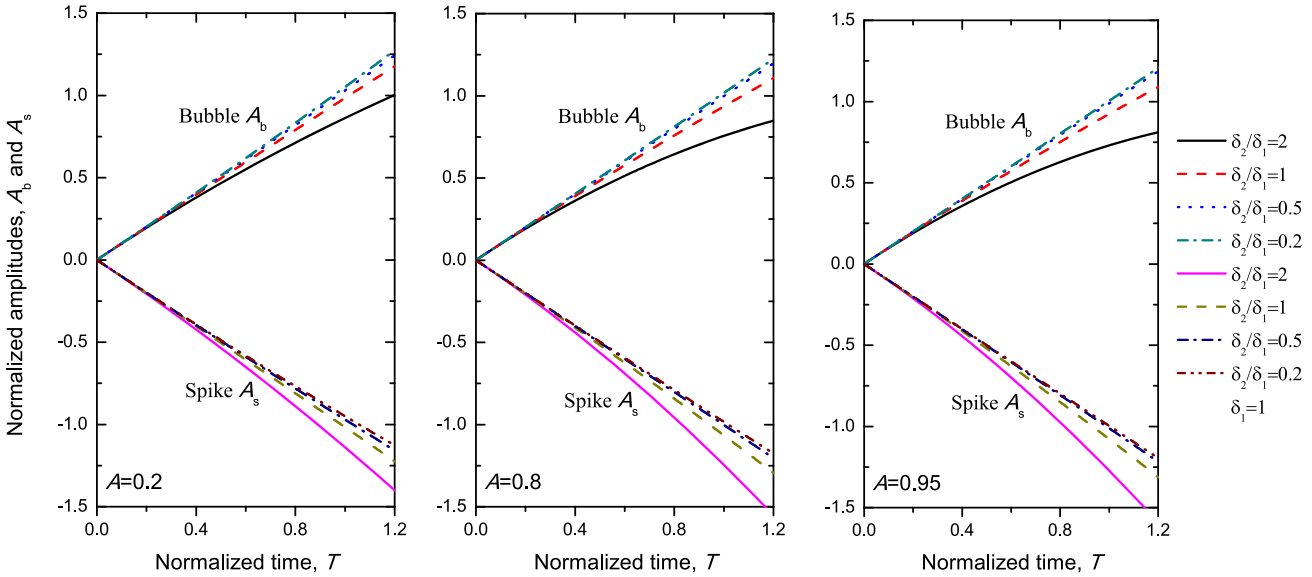

Figure 4. Normalized amplitudes of bubbles and spikes of the middle interface versus normalized time $T = kv_0t$ for different finite-thickness $\delta_2/\delta_1 = 2$, 1, 0.5, 0.2 and Atwood numbers $A = 0.2$ (left), $A = 0.8$ (middle) and $A = 0.95$ (right). The initial amplitude of the perturbation is $\hat{\varepsilon} = 1/1000$ and $\delta_1 = 1$.

In order to find out the reason why the amplitude of the bubble grows faster than the spike for some cases, we plot cosine functions of $Y_1 = 1.0\cos X$ and $Y_2 = 0.4\cos 2X$ in figure 5. If we select functions Y_1 and Y_2 as the fundamental mode, and the second harmonic at some special time, the function of the evolution interface will be $Y_1 + Y_2$, and the location of the bubble (spike) top will be at $X = 0$ ($X = \pi$). It is obvious that when the amplitude of the second harmonic is positive (such as 0.4 in this figure), the amplitude of the bubble will be larger than that of the spike; when it is negative (such as -0.4 opposite to this figure), the amplitude of the bubble will be less than the spike. Therefore, the amplitude of the second harmonic plays a leading role in the evolution of the bubble and the spike.

Whether the amplitude of second harmonic in equation (11) is positive or negative should be in our consideration. Due to $T > 0$, the amplitude is positive or negative, depending on the value of the B_2/B_1. Let $B_2/B_1 = 0$, one obtains the critical Atwood number

$$A_c = \frac{e^{2\zeta}[(1+e^4)(4\cosh\zeta - 3) - 2e(2+e(2e-3))\cosh 2\zeta]}{(e^{4\zeta}+1)[1+(e-1)e]^2 - (1+e^4)(2e^{\zeta} - 3e^{2\zeta} + 2e^{3\zeta})}, \quad (15)$$

Table 1. Law of the fluid-thickness effect on bubbles and spikes.

	$A = 0.2$		$A = 0.8(0.95)$	
	Bubbles ↑	Spikes ↓	Bubbles ↑	Spikes ↓
Case 1: ($\delta_2 \to \infty$) $\delta_1\downarrow$	⇓	⇑	⇓	⇑
Case 2: ($\delta_1 \to \infty$) $\delta_2\downarrow$	⇑	⇓	⇑	⇓
Case 3: finite-thickness $\delta_1 = \delta_2\downarrow$	⇑	⇓	⇑	⇓
Case 4a: finite-thickness $\delta_1 < \delta_2$	⇓	⇑	⇓	⇑
Case 4b: finite-thickness $\delta_1 > \delta_2$	⇑	⇓	⇑	⇓

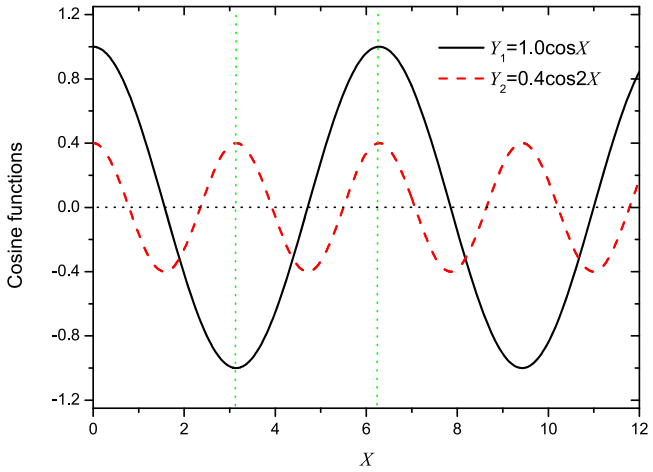

Figure 5. Cosine functions of $Y_1 = 1.0\cos X$ and $Y_2 = 0.4\cos 2X$.

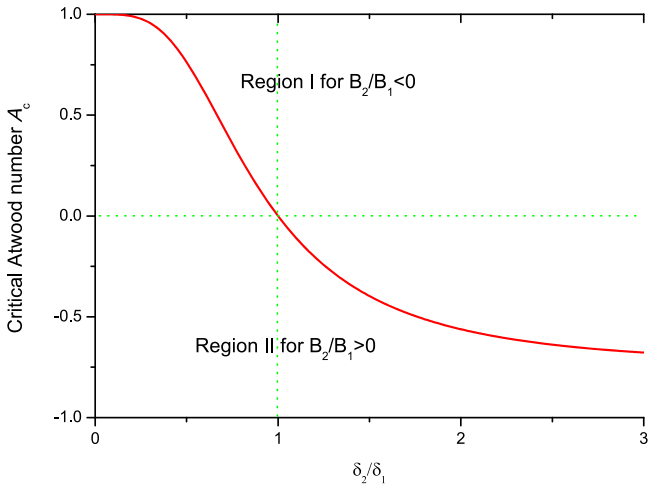

Figure 6. Critical Atwood number versus the ratio of the $\zeta = \delta_2/\delta_1$ with $\delta_1 = 1$.

where $\zeta = \delta_2/\delta_1$. As a result, we can conclude the following relationship: when $A > A_c$, $B_2/B_1 < 0$; when $A < A_c$, $B_2/B_1 > 0$; when $A = A_c$, $B_2/B_1 = 0$. The critical Atwood number A_c versus ζ is plotted in figure 6. The curve of the A_c separates the space of the parameters A and ζ into two regions: region I is for $B_2/B_1 < 0$ and region II is for $B_2/B_1 > 0$. That is to say, in region I, the amplitude of the second harmonic is negative, similar to the case of the classical RMI where the spike goes faster than the bubble; in region II, the amplitude of the second harmonic is positive, resulting in the spike growing slower than the bubble; when $A = A_c$, the amplitude of the second harmonic is always zero (i.e. the second harmonic vanishes), the interface, up to the second harmonic, consists just of the fundamental mode, and the amplitude of the bubble is the same as that of the spike. Additionally, for the $A > 0$ case, when $\zeta > 1$, the amplitude of the second harmonic is negative; when $\zeta < 1$, the amplitude of the second harmonic may be positive, depending on Atwood number. Therefore, the finite-thickness effect plays an important role in the amplitude evolution of the bubble and the spike, especially for $\zeta < 1$, i.e. the thickness of the heavy fluid is less than that of the light fluid.

In order to validate the finite-thickness effect, theory results are compared with the numerical simulation. For the two dimensional Euler equations of inviscid and compressible fluid dynamics, fifth-order finite difference WENO schemes with the third-order Runge–Kutta time discretization are used. In our numerical simulation, we set up the problem as follows: the computational domain is [0, 0.25] × [0, 2]; the location of the initial shock is at $y = 0.01$, and after the shock, the gas density is $\rho_0 = 0.2$, the velocity in the x-direction is $u = 0$, the one in the positive y-direction is $v = 2.700\,31$ and the pressure is $p = 3.5$. The shock with Mach number 1.0 moves in the positive y-direction, and goes successively through the gas with density $\rho_1 = 0.1$, the fluids with densities $\rho_2 = 2.0$ and $\rho_3 = 3.0$, and the gas with density $\rho_1 = 0.1$. The planar interface between the gas of density ρ_1 and the fluid of density ρ_2 is at $y = 0.05$, and the perturbed interface between the fluids of densities ρ_2 and ρ_3 is at $y = 0.3$, and another planar interface between the fluid of the density ρ_3 and the gas of the density ρ_1 is at $y = 0.55$. Before the shock, the pressure keeps constant $p = 1$ and the fluids and gas keep rest. The perturbed interface is set as $y = 0.3 + 0.001\cos(8\pi x)$, and then the perturbed wavelength is $\lambda = 0.25$. In this case, the shock travels two fluids with the same thickness $\delta = \lambda = 0.25$. The reflective boundary conditions are imposed for the $x = 0$ and $x = 0.25$ boundaries, and the free second-order boundary conditions are set at $y = 0$ and $y = 2$ boundaries. The mesh step is set as the uniform $h = 10^{-4}$. When an incident shock collides with the perturbed interface, it bifurcates into a transmitted shock, which moves in the direction of the incident shock, and a reflected wave, which moves in the opposite direction of the incident shock. When the reflected wave and transmitted shock leave the perturbed interface, the fluids are compressed and their densities become $\rho_l = 5.33$ and $\rho_h = 7.76$. That is to say, the Atwood number is $A = 0.186$. Because the whole perturbed interface move in the positive y-direction, it is

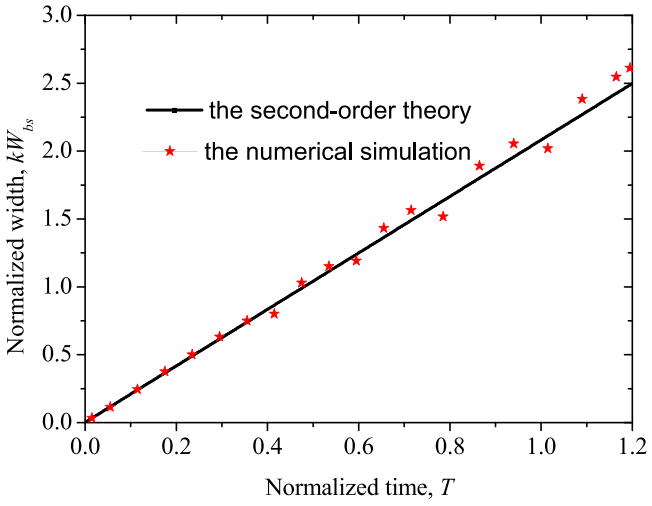

Figure 7. Comparison of the normalized width of mixing area full of two fluids from the second-order theory (line) and the numerical simulation (star) versus the normalized time $T = kv_0t$ for the same finite-thickness $\delta_1 = \delta_2 = k\lambda$ and Atwood numbers $A = 0.186$. The initial amplitude of the perturbation is $\hat{\varepsilon} = 8\pi/1000$.

inconvenient for us to track the amplitudes of the bubbles and spikes. Here, width of mixing area full of two fluids of densities ρ_h and ρ_l is defined as $W_{\mathrm{bs}} = |A_{\mathrm{b}} - A_{\mathrm{s}}|$. From figure 7, one finds that results from the second-order theory and the numerical simulation are in good agreement. The numerical simulation validates the second-order theory provided in this paper.

4. Conclusion

In classical RMI, the two semi-finite-thickness fluids are taken into account, however, in astronomical objects and engineering applications related to RMI the thickness of the fluids is finite. This paper mainly investigates the finite-thickness effect on the interface fingers including bubbles which are formed by the light fluid going in the heavy fluid, and spikes formed by the heavy fluid moving in the light fluid. In classical RMI, bubbles move slower than spikes. However, when the finite-thickness effect is taken into account, the character of the growth amplitudes of the bubbles and spikes is not always the same as the classical case. With time whether the amplitude of the spike is larger than that of the bubble depends on the Atwood number and the relationship of the thickness of the two fluids. When the thickness effect is considered, the amplitude of the spike keeps much larger than that of the bubble only for two cases. One is that the thickness of the heavy fluid $\delta_2 \to \infty$, and that of the light fluid δ_1 is finite, the other is that the two fluids are with finite-thickness, and they satisfy the relation $\delta_1 < \delta_2$ for arbitrary Atwood numbers. However, for more cases, the thickness effect of the fluids reduces the growth of the spikes and accelerates the bubbles, resulting in spikes traveling slower and bubbles doing faster. Therefore, the thickness effect of the fluids plays an important role in the amplitude evolution of bubbles and spikes at the weakly nonlinear stage of RMI.

Acknowledgments

The authors sincerely thank the anonymous reviewers for their valuable comments that have led to the present improved version of the original manuscript. This work was supported by National Natural Science Foundation of China (Nos. U1530261, 91852203, and 11472278), the Innovation Fund of Fundamental Technology Institute of All Value In Creation (No. JCY2015A005), the Natural Science Foundation of Sichuan Province (Nos. 18ZA0260, and 2018JY0454), the Natural Science Foundation of Mianyang Normal University (Nos. HX2017007, MYSY2017JC06 and MYSY2018T004), and the National High-Tech Inertial Confinement Fusion Committee.

References

[1] Richtmyer R D 1960 *Commun. Pure Appl. Math.* **13** 297
[2] Meshkov E E 1969 *Fluid Dyn.* **4** 101
[3] Velikovich A L *et al* 2000 *Phys. Plasmas* **7** 1662
[4] Matsuoka C and Nishihara K 2006 *Phys. Rev.* E **73** 055304(R)
[5] Haan S W 1995 *Phys. Plasmas* **2** 2480
[6] Nishihara B K *et al* 2010 *Phil. Trans. R. Soc.* A **368** 1769
[7] Zhou Y 2017 *Phy. Rep.* **720–722** 1
[8] Zhou Y 2017 *Phy. Rep.* **723–725** 1
[9] He X T and Zhang W Y 2007 *Eur. Phys. J.* D **44** 227
[10] He X T *et al* 2016 *Phys. Plasmas* **23** 082706
[11] Ye W H, Zhang W Y and He X T 2002 *Phys. Rev.* E **65** 057401
[12] Ye W H, Wang L F and He X T 2010 *Phys. Plasmas* **17** 122704
[13] Wang L F *et al* 2015 *Phys. Plasmas* **22** 082702
[14] Wang L F *et al* 2016 *Phys. Plasmas* **23** 052713
[15] Mikaelian K O 1996 *Phys. Rev.* E **54** 3676
[16] Wang L F *et al* 2014 *Phys. Plasmas* **21** 122710
[17] Velikovich A L and Schmit P F 2015 *Phys. Plasmas* **22** 122711
[18] Piriz S A, Piriz A R and Tahir N A 2017 *Phys. Rev.* E **95** 053108
[19] Dimonte G 1999 *Phys. Plasmas* **6** 2009
[20] Grove J W *et al* 1993 *Phys. Rev. Lett.* **71** 3473
[21] Alon U *et al* 1995 *Phys. Rev. Lett.* **74** 534
[22] Sohn S-I 2004 *Phys. Rev.* E **69** 036703
[23] Haan S W 1991 *Phys. Fluids* B **3** 2349
[24] Hecht J *et al* 1994 *Phys. Fluids* **6** 4019
[25] Zhang Q and Sohn S-I 1996 *Phys. Lett.* A **212** 149
[26] Sohn S-I 2003 *Phys. Rev.* E **67** 026301
[27] Wouchuk J G 2001 *Phys. Rev.* E **63** 056303
[28] Mügler C and Gauthier S 1998 *Phys. Rev.* E **58** 4548
[29] Rikanati A *et al* 1998 *Phys. Rev.* E **58** 7410
[30] Vandenboomgaerde M, Gauthier S and Mugler C 2002 *Phys. Fluids* **14** 1111
[31] Liu W H *et al* 2012 *Phys. Plasmas* **19** 072108
[32] Bender C M and Orszag S A 1978 *Advanced Mathematical Methods for Scientists and Engineers* (New York: McGraw-Hill)
[33] Mikaelian K O 1985 *Phys. Rev.* A **31** 410